HHS Public Access

Author manuscript

Neuroimage. Author manuscript; available in PMC 2021 October 01.

Published in final edited form as:

Neuroimage. 2020 October 01; 219: 117040. doi:10.1016/j.neuroimage.2020.117040.

The association of white matter free water with cognition in older adults

Joseph M. Gullett[a,*], **Andrew O'Shea**[a], **Damon G. Lamb**[a,b,c], **Eric C. Porges**[a], **Deirdre M. O'Shea**[a], **Ofer Pasternak**[d], **Ronald A. Cohen**[a], **Adam J. Woods**[a]

[a]Center for Cognitive Aging and Memory, McKnight Brain Institute, Department of Clinical & Health Psychology, University of Florida, 1225 Center Drive, Gainesville, FL, 32610-0165, USA

[b]Brain Rehabilitation Research Center, Malcom Randall VA Medical Center, 1601 SW Archer Road, Gainesville, FL, 32608, USA

[c]Department of Psychiatry, University of Florida, 100 S. Newell Dr., L4100, McKnight Brain Institute, Gainesville, FL, 32611, USA

[d]Departments of Psychiatry and Radiology, Brigham and Women's Hospital, Harvard Medical School, 1249 Boylston St., Boston, MA, 02215, USA

Abstract

Background: Extracellular free water within cerebral white matter tissue has been shown to increase with age and pathology, yet the cognitive consequences of free water in typical aging prior to the development of neurodegenerative disease remains unclear. Understanding the contribution of free water to cognitive function in older adults may provide important insight into the neural mechanisms of the cognitive aging process.

Methods: A diffusion-weighted MRI measure of extracellular free water as well as a commonly used diffusion MRI metric (fractional anisotropy) along nine bilateral white matter pathways were examined for their relationship with cognitive function assessed by the NIH Toolbox Cognitive Battery in 47 older adults (mean age = 74.4 years, SD = 5.4 years, range = 65–85 years). Probabilistic tractography at the 99th percentile level of probability (Tracts Constrained by Underlying Anatomy; TRACULA) was utilized to produce the pathways on which microstructural

*Corresponding author. Center for Cognitive Aging and Memory, McKnight Brain Institute, Department of Clinical & Health Psychology, University of Florida, 1225 Center Drive, Gainesville, FL, 32610-0165, USA. gullettj@phhp.ufl.edu (J.M. Gullett).

CRediT authorship contribution statement

Joseph M. Gullett: Conceptualization, Methodology, Formal analysis, Investigation, Writing - original draft, Writing - review & editing, Project administration, Funding acquisition. **Andrew O'Shea:** Methodology, Resources, Data curation, Writing - review & editing. **Damon G. Lamb:** Formal analysis, Investigation, Writing - review & editing, Visualization. **Eric C. Porges:** Writing - review & editing, Supervision, Funding acquisition. **Deirdre M. O'Shea:** Resources, Data curation, Writing - review & editing. **Ofer Pasternak:** Conceptualization, Methodology, Software, Writing - review & editing. **Ronald A. Cohen:** Validation, Writing - review & editing, Supervision, Funding acquisition. **Adam J. Woods:** Conceptualization, Validation, Formal analysis, Resources, Data curation, Writing - review & editing, Supervision, Project administration, Funding acquisition.

Declaration of competing interest

None.

Appendix A. Supplementary data

Supplementary data to this article can be found online at https://doi.org/10.1016/j.neuroimage.2020.117040.

characteristics were overlaid and examined for their contribution to cognitive function independent of age, education, and gender.

Results: When examining the 99th percentile probability core white matter pathway derived from TRACULA, poorer fluid cognitive ability was related to higher mean free water values across the angular and cingulum bundles of the cingulate gyrus, as well as the corticospinal tract and the superior longitudinal fasciculus. There was no relationship between cognition and mean FA or free water-adjusted FA across the 99th percentile core white matter pathway. Crystallized cognitive ability was not associated with any of the diffusion measures. When examining cognitive domains comprising the NIH Toolbox Fluid Cognition index relationships with these white matter pathways, mean free water demonstrated strong hemispheric and functional specificity for cognitive performance, whereas mean FA was not related to age or cognition across the 99th percentile pathway.

Conclusions: Extracellular free water within white matter appears to increase with normal aging, and higher values are associated with significantly lower fluid but not crystallized cognitive functions. When using TRACULA to estimate the core of a white matter pathway, a higher degree of free water appears to be highly specific to the pathways associated with memory, working memory, and speeded decision-making performance, whereas no such relationship existed with FA. These data suggest that free water may play an important role in the cognitive aging process, and may serve as a stronger and more specific indicator of early cognitive decline than traditional diffusion MRI measures, such as FA.

Keywords

Free water; Diffusion tensor imaging; Tractography; White matter; Cognitive aging; Cognitive function

1. Background

1.1. Brain and cognitive aging

Across the world, the elderly population is rapidly expanding (Bureau, 2009). In the United States, the 65 and older population is expected to double by the year 2050 (Bureau, 2009; Jacobsen et al., 2011). With increasing age, a variety of cognitive processes decline even in the absence of apparent neurological or neurodegenerative disease (Anton et al., 2015; Dotson et al., 2015; Woods et al., 2013, 2011). While language function is relatively well-preserved (e.g., vocabulary), learning and memory, working memory, speed of processing, executive function, and attention, as well as other abilities, steadily decline across the life span (Craik, F. I. M. & Salthouse, 2008; Salthouse, 1998). These cognitive functions that decline with age are collectively referred to as fluid cognition, while crystallized cognition is typically defined as abilities that either do not change or improve with age. The rates of fluid cognitive decline tend to be most pronounced in the seventh decade of life and beyond, and decline in fluid function in healthy elderly has been shown to have social and physical functional consequences (O'Shea et al., 2018). Cognitive decline late in life is associated with increased hospitalization, hospital re-admittance rates, mortality, loss of mobility, and, ultimately, loss of independence (Anton et al., 2015; Aubertin-Leheudre et al., 2015; Lövdén et al., 2005; Marioni et al., 2014; Woods et al., 2013, 2011). As the world's elderly

population increases, we are faced with a health system crisis, both in capacity limitations and financial burden (Brault, 2012; Bureau, 2009; Jacobsen et al., 2011). These difficulties highlight the need for markers sensitive to the cognitive aging process that will better inform our understanding of mechanisms underlying age-related decline, and may serve as potential targets for intervention.

1.2. Free water, cognitive aging, and disease

With brain atrophy comes microstructural changes within the white matter which are 1) related to lower cognitive performance, 2) most apparent within the prefrontal white matter connections early in the aging process, 3) apparent both in the whole brain and tract-specific, and 4) extend toward the posterior regions later in individuals of advanced age (Bennett, Ilana and Madden, David, 2014; Gunning-Dixon et al., 2009; Madden et al., 2012). The most common measure used to characterize white matter microstructure, fractional anisotropy (FA), typically demonstrates sensitivity as a marker of normal aging that declines prior to grey matter atrophy (Hugenschmidt et al., 2008). However, traditional measures of white matter microstructure such as FA may have inherent limitations. For example, increased extracellular space has been observed as a function of brain atrophy, and the presence of these spaces can limit the accuracy of diffusion magnetic resonance imaging (dMRI) due to partial volume effects (Fjell et al., 2008). In other words, the accuracy of FA as a metric can be altered from partial volume effects depending upon the curvature, thickness, and orientation of the pathway in a given voxel (Vos et al., 2011). Further, partial volume effects may be more evident in the outermost portions of white matter pathways having an increased likelihood of including higher proportions of CSF, or even grey matter, within a given voxel. To partially address this potential confound, free water imaging from diffusion-weighted MRI has been proposed as a method to estimate and eliminate the effect of extracellular free-water on the dMRI signal (Pasternak et al., 2009).

Free water is defined as water molecules that are free to diffuse and do not experience restriction or hindrance. In conventional dMRI acquisitions, within a given brain voxel free water can be found in the extracellular space, which includes cerebrospinal fluid (CSF), interstitial space, or plasma. Diffusion imaging of free water was originally described as a method for reducing the partial volume effects of freely diffusing extracellular water within white matter to produce a more accurate estimate of the white matter microstructure (Pasternak et al., 2009). Increases in free water levels are thought to reflect accumulation of extracellular water, which may occur due to processes such as atrophy, edema, or breakdown of myelin cell membranes that would typically restrict diffusion of water (Maier-Hein et al., 2015; Ofori et al., 2015; Pasternak et al., 2016, 2015; 2014, 2012; 2009; Weston et al., 2015). Subsequent research on the topic has found that free water levels have a stronger association with age than traditional diffusion tensor imaging (DTI) measures (Chad, J.A., Pasternak, O., Salat, D.H., Chen, 2018). Recent longitudinal studies of elderly subjects found that free water-adjusted measures of white matter microstructure are more reliable, and better predict markers of aging and disease-specific pathology than white matter investigations performed without correction for partial volume effects (Albi et al., 2017; Chad, J.A., Pasternak, O., Salat, D.H., Chen, 2018; Maier-Hein et al., 2015). In subjects with neurodegenerative disease, progressive increases in free water levels are observed at each

stage throughout the disease progression from healthy, to mild cognitive impairment (MCI), to Alzheimer's disease (AD) (Montal et al., 2018).

At present, the functional consequences of free water in typical aging without neurodegeneration remain unknown. The association of free water and cognition in a sample of cognitively diverse individuals was recently examined as a function of free water across the entire brain in relation to cognition (Maillard et al., 2019). The authors found global associations of whole-brain free water to be positively related to the Clinical Dementia Rating scale as well as broad measures of cognitive functioning and their change over time. However, more detailed and specific associations between free water along white matter pathways and cognitive function have yet to be examined in typical aging. Thus, the current study sought to elucidate the relationship between free water, age, and cognitive performance in older adults without neurodegenerative disease in order to better understand the unique role of free water in cognitive aging. Utilizing a sample of 47 typically-aging older adults, we studied the relationship between free-water across nine white matter pathways and neurocognitive function. as measured by the comprehensive NIH Toolbox (NIHTB) Cognitive Battery (Akshoomoff et al., 2013; Bauer and Zelazo, 2013; Weintraub et al., 2013). We hypothesized that,1) Free water values across a majority of the investigated white matter tracts would be greater with increasing age, 2) higher free-water values would be associated with poorer cognitive performance in fluid but not crystallized cognitive performance, and 3) free water would be the strongest correlate of cognitive aging, followed by a free water-adjusted traditional diffusion metric (e.g. Free Water-corrected Fractional Anisotropy), and the traditional diffusion metric alone (Fractional Anisotropy).

2. Methods

2.1. Participants

Forty-seven older adults (57.4% female) were recruited from the north-central Florida community. The study protocol was reviewed and approved by the University of Florida Institutional Review Board and all participants willingly provided written informed consent to participate in the study. Participants had a mean age of 74.4 years (SD = 5.4 years, range = 65–85 years) and an average of 16.6 years of education (SD = 2.4 years, range = 12–20 years) (Table 1). Participants were screened for dementia using the Montreal Cognitive Assessment (MoCA; M = 25.8, SD = 2.5, range = 20–30) (Nasreddine et al., 2005), assessment of normative neuropsychological values on the NIH Toolbox (greater than 1 SD deficit in a cognitive domain on demographically corrected scores), and self-reported medical history. None of the participants carried previous diagnoses of mild cognitive impairment or Alzheimer's disease. Participants were excluded for pre-existing neurological or major psychiatric brain disorders, MRI contraindications, diagnosis with a neurodegenerative brain disease (i.e. Alzheimer's, Parkinson's), and self-reported difficulty with thinking and/or memory.

2.2. Neurocognitive measures

The NIH Toolbox Cognitive Battery was administered as a brief assessment of neurocognitive function (Akshoomoff et al., 2013; Bauer and Zelazo, 2013; Weintraub et al.,

2013). Subtests of the NIHTB Cognitive Battery are divided into two composite measures of global cognitive function: 1) fluid cognitive abilities (abilities that change with age) and crystallized cognitive abilities (abilities that do not typically change with age). The fluid cognition composite is composed of the following tasks: Dimensional Change Card Sort, Flanker, Picture Sequence Memory, List Sorting, and Pattern Comparison. The crystallized cognition composite is composed of the Picture Vocabulary Test and the Oral Reading Recognition Test. More information about these measures and the creation of the two index scores can be found in the original work of Weintraub et al. (Weintraub et al., 2013). For the purposes of this study, the unadjusted crystallized and fluid composite scaled scores were utilized for analyses with age, education, and gender as covariates. For planned follow-up analyses, raw performance on the various subtests comprising these index measures were used with age, education, and gender as regression covariates. Use of these adjusted or raw scores in analyses, respectively, when combined with diffusion metrics allows for equitable comparisons. Briefly in regard to cognitive performance, we observed the typical age-related decline in fluid cognitive performance with advancing age, and a flat-to-slightly increasing relationship between age and crystallized cognitive performance.

2.3. Neuroimaging acquisition

All participants were imaged in a Philips 3T scanner (Achieva; Philips Healthcare), at the McKnight Brain Institute (University of Florida, Gainesville, Florida) with a 32-channel receive-only head coil. A high-resolution T1 weighted MPRAGE sequence and a 64-direction high angular resolution diffusion-weighted imaging sequence were performed. Scanning parameters for the structural T1 consisted of: voxel size = 1 mm isotropic; TE = 3.2 ms; TR = 7.0 ms; FOV = 240×240; Number of slices = 170; acquired in a sagittal orientation. We also obtained diffusion imaging data with a spin-echo prepared echo planar image (Poustchi-Amin et al., 2001) using the following parameters: TR/TE = 4840/86 ms, 1 b = 0 scan (without diffusion weighting), 64 gradient directions with diffusion weighting 1000 s/mm2, isotropic resolution of 2.0 mm, field of view (FOV) of 224 mm × 224 mm, and 74 slices, covering the entire brain, with diffusion gradients distributed following a scheme of electrostatic repulsion (Jones et al., 1999).

2.4. Neuroimaging processing

2.4.1. T1-weighted imaging—

T_1-weighted images were processed through the FreeSurfer version 6.0.0 software. More information on the Bayesian inference methods and reliability of results utilizing Freesurfer software can be found in the original work by Fischl et al. and follow-up work by Jovicich et al., respectively (Fischl et al., 2002; Jovicich et al., 2009). The white matter segmentation results were manually inspected, slice-by-slice, and control points were created to ensure accurate estimation of white matter borders throughout the brain. Maps were then re-processed with these control points, producing results that should better resemble previous maps that have been validated against histological measures (Cardinale et al., 2014) and manual segmentation in specific brain regions (Morey et al., 2009). The resulting segmentation data were then utilized for further analysis in conjunction with the dMRI data described below.

2.4.2. Diffusion modeling and parameter calculation—A two compartment model was used (Pasternak et al., 2009) to separately model water molecules in the vicinity of brain tissue (the tissue compartment) and water molecules that are freely diffusing without being hindered or restricted by tissue membranes (the free water compartment). This model was fitted using a regularized minimization procedure implemented in Matlab (Pasternak et al., 2009), resulting in a free water map, which is a quantitative metric of the free water fraction in each voxel. Further, a fractional anisotropy (FA)(Basser and Pierpaoli, 1996) map was calculated from the tissue compartment to produce a free water adjusted FA. In order to produce the FA map, the diffusion data were corrected for eddy current distortions, brain extracted, and tensor calculations were performed using the Functional MRI of the Brain Software Library (FSL) *dtf*i*t* tool (Fsl, 2006). FA was chosen as a comparative metric to the free water metric as it is a commonly-used diffusion parameter that represents the overall integrity of the white matter. To do so, FA incorporates several physical parameters of water diffusion in each voxel as derived by the three principle eigenvalues and as seen in the FA equation (Özarslan et al., 2005):

$$FA = \sqrt{1/2}\frac{\sqrt{(\lambda_1 - \lambda_2)^2 + (\lambda_2 - \lambda_3)^2 + (\lambda_3 - \lambda_1)^2}}{\sqrt{\lambda_1^2 + \lambda_2^2 + \lambda_3^2}}$$

2.4.3. Diffusion tensor imaging—TRACULA (TRActs Constrained by UnderLying Anatomy) is a neuroimaging tool which was chosen because it allows automatic reconstruction of common major white-matter pathways derived from diffusion-weighted MRI (Yendiki, 2011). The primary analysis utilized dMRI data that were processed through the default TRACULA pipeline, which utilizes the *trac-all* command as well as correction for eddy current distortions, brain extraction, tensor calculation, and affine registration and normalization to the MNI-152 template using FSL's flirt (Fsl, 2006; Jenkinson et al., 2002; Jenkinson and Smith, 2001). This process results in the reconstruction of 18 commonly studied white matter pathways using the probability distributions of voxel-based fiber orientations along each tract. The resulting pathways included forceps major (fmajor) and minor (fminor) of the corpus callosum, and bilateral pathways for the anterior thalamic radiation (ATR), cingulate gyrus cingulum bundle (CCG), cingulate gyrus angular bundle (CAB), corticospinal tract (CST), inferior longitudinal fasciculus (ILF), superior longitudinal fasciculus temporal bundle (SLFt), superior longitudinal fasciculus parietal bundle (SLFp), and uncinate fasciculus (UNC). Pathways for each participant were manually inspected for gross reconstruction errors or missing pathways and corrected (necessitated for one pathway across two participants [CAB and UNC]) as needed such that no missing data were present The *Average Center* pathway data represent the pathway in which each adjacent voxel in the path has a 99% probability of being the next true fiber in the pathway, based on diffusion characteristics. This measure, as opposed to the standard output tract, provides the highest level of anatomical feasibility for the resulting pathways, and the primary tract measure utilized in this study.

2.4.4. Free water and fractional anisotropy extraction from regions of interest—Using the free water, FA, and free water-adjusted FA maps as the base image and

the *Average Center* pathway as the mask (99% probability connection), mean diffusion (FA, free water) values across each of the nine *Average Center* pathway masks were calculated for each participant using the *fslmaths* tool (Jenkinson et al., 2012). Using the *Average Center* data serves to increase confidence that the pathways examined are indeed representative of true white matter neuroanatomy and minimize overlap with cerebrospinal fluid (CSF), which would be identified as partial volume in the extracted free water values (Pasternak et al., 2009). The default TRACULA tract output and the 99th percentile probability pathway are presented together along the corticospinal tract of a representative participant for visualization (Fig. 1). In order to further reduce the possibility of false discovery, the diffusion values for each hemisphere of the sixteen *Average Center* pathways were averaged together to create eight bilateral pathway values. Later analyses determined data across the SLFt and SLFp pathways to be highly co-linear and statistically indistinguishable, and as such, the values for these two physically co-located pathways were collapsed into a single bilateral variable (SLF). Thus, when combined with the two collosal pathways (fmajor and fminor), the present study utilized a total of nine final pathways per diffusion modality, as in previous research by our group (Gullett et al., 2018).

2.5. Statistical analyses

Statistical analyses were performed with SPSS Statistics v24.0 (IBM, 2016). Tables and statistical figures were created using SPSS as well as R 3.3.3 statistics package (R Development Core Team, 2016), and ggplot 2.2.1 (Wickham, 2017). All demographic and neurocognitive variables of interest met the requirements of normality specified by the GLM model in terms of skewness and kurtosis, as z-skew or z-kurt values did not exceed normal limits to necessitate normalization. There were no missing demographic or neurocognitive data across the included participants. Outlier diffusion values (greater than ± 3SD from the mean) extracted from the probabilistic tractography pathways were normalized with Winsorization, which is a common practice (Jones et al., 2017; Templeton, 2011). Winsorization was only necessitated for one pathway (CCG) belonging to one participant.

The primary analysis examining the relationship of cognition and diffusion values averaged across the entire *Average Center* path for each bilateral tract was performed. The formula for this regression equation is as follows:

$$CogMeasure = B_{intercept} + B_{age}age + B_{edu}edu + B_{male\ sex}sex + B_{female\ sex}\ sex + B_{diffusion}diffusion$$

In this analysis, a series of linear regressions were performed to determine the relationship of three diffusion metrics to the two unadjusted NIH Toolbox composite cognitive indices (Fluid cognition and Crystallized cognition), with covariates of age, education, and gender. The dependent variable (DV) was the cognitive index and the independent variables (IVs) included the three covariates (age, education, gender) along with the average diffusion value across the tract of interest. Lastly, secondary analyses were performed for those bilateral pathways that were significantly related to cognitive functioning to determine the specific contribution of each NIH Toolbox cognitive subtest. Left and right hemisphere data were also examined for their individual contributions to each cognitive subtest with additional regressions. These analyses allowed for determination of specificity of the relationships in

regard to the neuropsychological functions associated with each anatomical pathway. Each linear regression investigating the relationship between cognitive performance and the mean diffusion value of each pathway was corrected for False Discovery Rate (FDR) at a p-value threshold of $p < .05$ using the Benjamini and Hochberg method considering a total of nine pathways examined, which consistent with and perhaps even more conservative than similar recent investigations (Boots et al., 2019; Chopra et al., 2018; Luo et al., 2019). Investigations involving the hemispheric contributions of each specific subtest were corrected similarly for a total of nine regressions given that both hemispheres were entered as IVs into the model for each pathway. For display purposes as an attempt to deal with potential multi-collinearity of variables, we provide values from a partial correlation (ρ) independently correcting both the diffusion and cognitive variables for age, education, and gender. These values provide visualization of the unique relationship between a single diffusion metric and cognitive performance after removing the effect of latent variables (e.g. age, education, and gender). Lastly, QQ plots were visualized for the standardized and unstandardized residuals of all regressions performed, which revealed no evidence of abnormality or deviation from the regression line which would require further investigation with a Kolmogorov-Smirnov test.

3. Results

3.1. Sample demographics

One-way ANOVA determined MoCA performance was significantly higher for female participants ($M = 26.7$, $SD = 2.54$) than males ($M = 24.6$, $SD = 1.90$; $F[1,46] = 9.78$, $p = .003$). Otherwise, there were no significant differences between male and female participants on any of the demographic, cognitive, or neuroimaging-based measures utilized in this study. The majority of the sample was right-handed, and given that the language-related measures administered were isolated to the crystallized composite and were 1) not speed-dependent tasks, and 2) investigated in relation to bilateral hemisphere neuroimaging data, participant handedness is of minimal concern regarding potential influence on the findings.

3.2. Age and white matter diffusion across TRACULA-derived pathways

In general, diffusion data demonstrate the commonly described pattern of decreasing white matter integrity (higher free water) with increasing age. When utilizing the 99th percentile pathway data derived from TRACULA, covarying for education, gender, and applying an FDR correction ($p < .05$), there was a significant positive relationship between age and mean free water across one of the nine pathways examined; the ATR ($R^2 = 0.20$, $p = .027$). Three additional pathways demonstrated trends toward significance after FDR correction, including the CAB ($R^2 = 0.12$, $p = .081$), ILF ($R^2 = 0.14$, $p = .081$), and the SLF ($R^2 = 0.12$, $p = .081$). There was no significant association between age and mean FA or mean free water-adjusted FA across any of the nine pathways examined after FDR correction (Table 2).

3.3. Free water values and cognitive performance

When including in the regression model variables of age, education, and gender, fluid and crystallized cognition were examined for their relationship with average free water values across each of the nine bilateral 99th percentile probability pathways produced by

TRACULA. After applying FDR correction, lower fluid cognitive performance on the NIH toolbox was significantly related to higher mean free water values across four of the nine bilateral pathways, including the CAB (R^2 = 0.35, β = −0.42, FDR-p = .027), CCG (R^2 = 0.29, β = −0.33, FDR-p = .045), CST (R^2 = 0.28, β = −0.33, FDR-p = .045), and SLF (R^2 = 0.30, β = −0.35, FDR-p = .045), (Table 3). There was no association between crystallized cognition and free water diffusion after FDR correction, though trends were observed for the CAB (R^2 = 0.35, β = −0.35, p = 0.035, FDR-p = 0.19) and ILF (R^2 = 0.37, β = −0.31, p = 0.058, FDR-p = 0.19) pathways. For visualization of these results, values from a partial correlation (ρ) independently correcting both the diffusion and cognitive variables for age, education, and gender are displayed in Fig. 2.

3.4. Fractional anisotropy and cognitive performance

When covarying for age, education, and gender, neither fluid cognition nor crystallized cognition were associated with mean FA or with mean free water-adjusted FA across any of the nine bilateral white matter pathways. A trending association for lower fluid cognitive performance with lower mean FA across the Forceps Major of the corpus callosum was observed (R^2 = 0.28, β = 0.30, p = 0.03, p-FDR = 0.20). Otherwise, neither FA nor free water-adjusted FA were related to cognitive performance across the remaining pathways, though directional trends were consistently positive such that higher FA or FW-adjusted FA were associated with better fluid cognitive performance (Supplemental Table 3).

Planned follow-up analyses to determine the specific Fluid Cognition subtest or subtests driving these relationships were then performed, using subtest performance as the DV, mean free water across each of the four significant pathways as the IV, and covariates of age, education, and gender. These analyses revealed that higher mean free water values across the CAB was significantly associated with decreasing performance on the List Sorting memory task (β = −0.44, FDR-p = .015), higher mean free water across the CCG was associated with lower Picture Sequencing memory performance (β = −0.41, FDR-p = .030), higher mean free water across the CST was associated with lower Flanker performance (β = −0.49, FDR-p = .005), and higher mean free water across the SLF was associated with lower List Sorting memory (β = 0.38, FDR-p = .033) (Table 3; Fig. 3).

4. Discussion

The present investigation extends age-related associations in extracellular free water to cognitive function and white matter tracts obtained using an innovative probabilistic tractography approach. When examining white matter microstructure across the core pathway of nine major white matter tracts, which serves to minimize partial volume with CSF and grey matter, we demonstrate that higher free water values within the core white matter pathway are related to poorer fluid cognitive function. Further, there appears to exist a strong hemisphere-specific, structure-function relationship between free water within specific pathways and their associated neurocognitive function.

When examining the 99th percentile (*Average Center)* core white matter pathway produced by TRACULA, mean free water across four tracts was a significant predictor of fluid cognitive ability, while a traditional measure of diffusion (FA) was not. The association

between higher mean free water across these four pathways and the neuropsychological subtest contributing to the effect was specific to the functions required of the related cognitive task. Significant associations between poorer fluid cognitive functioning and higher mean free water values were observed across the core pathway of the angular bundle of the cingulate gyrus (CAB), the cingulum bundle of the cingulate gyrus (CCG), the corticospinal tract (CST), and the superior longitudinal fasciculus (SLF). Interestingly, the cognitive subtasks associated with higher mean free water across the CAB and CCG were those related to memory and working memory functions (Picture Sequencing and List Sorting, respectively), as might be expected for these frontotemporal pathways with hippocampal involvement (Bubb et al., 2018; Schmahmann and Pandya, 2009). Similar task-related specificity was seen for the association between higher mean free water values across the CST, a large-bundle cortical-motor pathway emanating from the brainstem, and poorer Flanker performance, an inhibitory-reaction time task with a strong psychomotor decision-making component. Even further, these findings were hemisphere specific, such that tasks involving language (List Sorting) were more significant for the left hemisphere portion of the tract, while largely non-verbal measures (Picture Sequencing, Flanker) were more significant for the right hemisphere portion of the associated pathway. These findings extend the white matter and cognitive aging literature, and provide unique evidence of a physiological process that appears to play a role in cognitive aging.

While previous studies have shown free water and free water-adjusted FA to be stronger correlates of aging than traditional FA (Chad, J.A., Pasternak, O., Salat, D.H., Chen, 2018), mean free water was only associated with age across the anterior thalamic radiation (ATR), after multiple comparison correction. Further, no association existed between age and mean FA nor mean free water-adjusted FA when utilizing the core white matter pathway produced by TRACULA. Lack of such associations are potentially due to the use of the relatively small core pathway along the white matter tract which may not be sensitive enough to demonstrate age-related white matter integrity effects in a healthy aging cohort. This use of a healthy aging cohort may have further implications for the lack of findings as well, as free water-corrected indices have been shown to represent tissue degeneration and alterations to the myelin sheath in previous studies (Pasternak et al., 2015). As grey matter regions deteriorate, white matter typically declines concurrently in those of advanced age (Brickman et al., 2005; Raz et al., 2005; Salat et al., 1999), such as those participants utilized in the present study (ages 65–85). Further, much like in the present study, these associations appear in the cingulate and dorsolateral frontal regions of the brain (Brickman et al., 2005). Degradation of the white matter pathway is not likely to be uniform and may demonstrate an outside-in deterioration pattern, though limited examination of this potential pattern has been performed in the literature. This suggests that the use of microstructural white matter integrity across a larger, sample-based calculation of the white matter bundle as typically done in research (e.g. TBSS) may be appropriate for the examination of disease- or aging-related changes. However, it is possible that these approaches lack the sensitivity to detect changes in microvasculature or potential inflammation in normal aging given the confounded dMRI signal from CSF, grey matter, and partial volume averaging typically present along the outer edge of white matter pathways. For example, a recent study demonstrated a strong association between higher free water and lower cognitive

performance in an MCI cohort but a decreasing utility of TBSS-examined free water as disease progression increased (Ji et al., 2019). We demonstrate that in the context of healthy aging, the use of a similar method utilizing the probabilistically-derived 99th percentile core white matter pathway retains both an age and cognitive function relationship that is specific to the neuropsychological function of a given pathway.

It has been demonstrated that changes in white matter as measured by FA in normal aging typically occurs along an anterior-posterior gradient, where earlier changes are seen in the frontal versus posterior white matter and correlating with declines in frontally- or attentionally-mediated cognitive functions (Gunning-Dixon et al., 2009). The present study demonstrates a higher value of free water with increased age along mostly frontal and temporal regions, and these associations were also related to lower performance on frontally-mediated cognitive tasks. These findings demonstrate a strong coupling of free water and frontally-mediated cognitive performance as compared to FA, suggesting that free water may serve as a more sensitive early marker of age-related cognitive decline than traditional dMRI measures when extracted from a probabilistically-derived pathway across the core white matter connection.

While direct data linking free water to physiological changes is lacking, prior work has suggested free water may be a marker of early axonal degeneration (Hoy et al., 2017a,b), or a potential marker of neuroinflammatory processes (Albi et al., 2017; Maier-Hein et al., 2015; Pasternak et al., 2015, 2014, 2012, 2009). If true, age-related increases in free water fraction across major white matter pathways may represent a chronic consequence of the aging process, and may even be a contributing factor to physiological decline underlying the cognitive aging process. However, the fact that the relationship between free water and cognitive function remained significant even after accounting for chronological age, education, and gender suggests that extracellular free water has broad-ranging implications for cognitive function; and may possibly represent a more insidious process. More biomarker studies are needed to determine the association of the free water metric and early pathological neuroinflammatory and neurodegenerative processes. Should future studies establish this link, the less-invasive nature of free water data collection can be utilized, and effective interventions to target such processes can be developed and tested in an attempt to slow the rate of cognitive aging. The data presented in the current study represent an additional link in the growing chain of literature investigating the subtle changes in cognitive function across non-pathologically aging populations. In this regard, additional research investigating cognitive function relationships to differences in extracellular free water across AD, MCI, and healthy aging will provide important insight into a potentially useful biomarker for cognitive decline.

This study has a number of limitations worth consideration. The sample size of forty-seven older adults is relatively small. We attempted to address this limitation by considering only the findings of strongest statistical significance with an appropriately-sized FDR correction at $p < .05$ based on the number of pathways examined. It is possible that, given the nine pathways were examined for their association with both fluid and crystalized cognitive function, this level of correction is insufficient to warrant significance. However, we feel the presented results are quite relevant given the high level of specificity for the resulting

significant pathways and their associated neurocognitive functions. Regardless, these factors highlight the need for larger, longitudinal studies of free water change in typical aging, as well as throughout the trajectory of neurodegenerative disease states. Further, the present study utilizes single-shell dMRI data, which requires a regularized minimization to estimate the model parameters. With more elaborated dMRI acquisitions, the regularization assumptions can be relaxed, free water can be more reliably estimated (Hoy et al., 2017a,b; Pasternak et al., 2014), and confounding effects such as blood plasma (Rydhög et al., 2017) or relaxation times (Rydhög et al., 2019) can be removed. Registration inaccuracies may also cause the inclusion of mostly-CSF voxels which can bias the free water measurement. However, the current study used the 99% probability core white matter pathway for each tract of interest to minimize potential influence from CSF. While it is impossible to rule out an influence of confounding CSF, the approach taken here serves to limit potential influence.

5. Conclusions

The purpose of this investigation was to describe in a typically-aging cohort the specific association between free water in white matter and cognitive function. Our results demonstrate that examining white matter microstructure in a manner that is relatively free of the confounds of CSF and grey matter infringement may improve the specificity of cognitive associations with a given a probabilistically-derived core white matter tract in typically-aging older adults. Specifically, we show that higher extracellular free water across the core of the cingulate gyrus, corticospinal tract, and superior longitudinal fasciculus white matter pathways are associated with poorer fluid cognitive function in normal older adults. Higher mean free water fraction across these pathways appears to be sensitive to lower hemisphere-specific cognitive functions of working memory, inhibitory reaction time, and memory processes; even when accounting for the effect of age, education, and gender. Thus, our data demonstrate that the presence of free water within white matter is not only greater with advanced age, but has functional consequences for cognition. With further research and greater understanding of the physiological process resulting in age-related increases of free water, this measure may serve as a modifiable target for intervention.

Supplementary Material

Refer to Web version on PubMed Central for supplementary material.

Funding

This work was supported in part by the McKnight Brain Research Foundation, 1Florida Alzheimer's Disease Research Center, Gainesville, FL, USA (grant number AG047266 to JG) and the National Institutes of Health (grant numbers U01-AA020797-09 to JG; K01AG050707-A1 and R01AG054077 to AW; R01AG042512 and P41EB015902 to OP).

References

Akshoomoff N, Beaumont JL, Bauer PJ, Dikmen SS, Gershon RC, Mungas D, Slotkin J, Tulsky D, Weintraub S, Zelazo PD, Heaton RK, 2013 VIII. NIH Toolbox Cognition Battery (CB): composite scores of crystallized, fluid, and overall cognition. Monogr. Soc. Res. Child Dev 78, 119–132. 10.1111/mono.12038. [PubMed: 23952206]

Albi A, Pasternak O, Minati L, Marizzoni M, Bartr es-Faz D, Bargallo N, Bosch B, Rossini PM, Marra C, Müller B, Fiedler U, Wiltfang J, Roccatagliata L, Picco A, Nobili FM, Blin O, Sein J, Ranjeva JP, Didic M, Bombois S, Lopes R, Bordet R, Gros-Dagnac H, Payoux P, Zoccatelli G, Alessandrini F, Beltramello A, Ferretti A, Caulo M, Aiello M, Cavaliere C, Soricelli A, Parnetti L, Tarducci R, Floridi P, Tsolaki M, Constantinidis M, Drevelegas A, Frisoni G, Jovicich J, 2017 Free water elimination improves test–retest reproducibility of diffusion tensor imaging indices in the brain: a longitudinal multisite study of healthy elderly subjects. Hum. Brain Mapp 10.1002/hbm.23350.

Anton SD, Woods AJ, Ashizawa T, Barb D, Buford TW, Carter CS, Clark DJ, Cohen RA, Corbett DB, Cruz-Almeida Y, Dotson V, Ebner N, Efron PA, Fillingim RB, Foster TC, Gundermann DM, Joseph A-M, Karabetian C, Leeuwenburgh C, Manini TM, Marsiske M, Mankowski RT, Mutchie HL, Perri MG, Ranka S, Rashidi P, Sandesara B, Scarpace PJ, Sibille KT, Solberg LM, Someya S, Uphold C, Wohlgemuth S, Wu SS, Pahor M, 2015 Successful aging: advancing the science of physical independence in older adults. Ageing Res. Rev 24, 304–327. 10.1016/j.arr.2015.09.005. [PubMed: 26462882]

Aubertin-Leheudre M, Woods AJ, Anton S, Cohen R, Pahor M, 2015 Frailty clinical phenotype: a physical and cognitive point of view. Nestle Nutr. Inst. Workshop Ser 83, 55–63. 10.1159/000382061. [PubMed: 26484671]

Basser PJ, Pierpaoli C, 1996 Microstructural and physiological features of tissues elucidated by quantitative-diffusion-tensor MRI. J. Magn. Reson., Ser. B 111, 209–219. 10.1006/jmrb.1996.0086. [PubMed: 8661285]

Bauer PJ, Zelazo PD, 2013 NIH toolbox cognition battery (CB): summary, conclusions, and implications for cognitive development. Monogr. Soc. Res. Child Dev 78, 133–146. 10.1111/mono.12039. [PubMed: 23952207]

Bennett Ilana J., Madden David J., 2014 Disconnected aging: cerebral white matter integrity and age-related differecnes in cognition. Neuroscience. 10.1016/j.biotechadv.2011.08.021 (Secreted).

Boots EA, Zhan L, Dion C, Karstens AJ, Peven JC, Ajilore O, Lamar M, 2019Cardiovascular disease risk factors, tract-based structural connectomics, and cognition in older adults. Neuroimage. 10.1016/j.neuroimage.2019.04.024.

Brault MW, 2012 Americans with disabilities: 2010 - household economic studies In: Current Population Reports. U.S. CENSUS BUREAU - U.S. Department of Commerce -Economics and Statistics Administration, pp. 70–131.

Brickman AM, Buchsbaum MS, Shihabuddin L, Haznedar M, Newmark RE,Brand J, Chen AD, Hazlett EA, 2005 Age-associated change in orbital, cingulate, and dorsolateral frontal lobe gray and white matter volume. J. Int. Neuropsychol. Soc 11, 176.

Bubb EJ, Metzler-Baddeley C, Aggleton JP, 2018 The cingulum bundle: anatomy, function, and dysfunction. Neurosci. Biobehav. Rev 10.1016/j.neubiorev.2018.05.008.

Bureau USC, 2009 An Aging World : 2008. Aging (Albany. NY) https://doi.org/P95/09-1.

Cardinale F, Chinnici G, Bramerio M, Mai R, Sartori I, Cossu M, Lo Russo G, Castana L, Colombo N, Caborni C, De Momi E, Ferrigno G, 2014 Validation of FreeSurfer-estimated brain cortical thickness: comparison with histologic measurements. Neuroinformatics 12, 535–542. 10.1007/s12021-014-9229-2. [PubMed: 24789776]

Chad JA, Pasternak O, Salat DH, Chen JJ, 2018 Re-examining age-related differences in white matter microstructure with free-water corrected diffusion tensor imaging. Neurobiol. Aging 72.

Chopra S, Shaw M, Shaw T, Sachdev PS, Anstey KJ, Cherbuin N, 2018 More highly myelinated white matter tracts are associated with faster processing speed in healthy adults. Neuroimage 10.1016/j.neuroimage.2017.12.069.

Craik FIM, Salthouse TA (Eds.), 2008 The Handbook of Aging and Cognition, third ed. Psychology Press 10.1002/acp.1505.

Dotson VM, Szymkowicz SM, Sozda CN, Kirton JW, Green ML, O'Shea A, McLaren ME, Anton SD, Manini TM, Woods AJ, 2015 Age differences in prefrontal surface area and thickness in middle aged to older adults. Front. Aging Neurosci 7, 250 10.3389/fnagi.2015.00250. [PubMed: 26834623]

Fischl B, Salat DH, Busa E, Albert M, Dieterich M, Haselgrove C, Van Der Kouwe A, Killiany R, Kennedy D, Klaveness S, Montillo A, Makris N, Rosen B, Dale AM, 2002 Whole brain

segmentation: automated labeling of neuroanatomical structures in the human brain. Neuron 33, 341–355. 10.1016/S0896-6273(02)00569-X. [PubMed: 11832223]

Fjell AM, Westlye LT, Greve DN, Fischl B, Benner T, Van Der Kouwe AJW, Salat D, Bjørnerud A, Due-Tønnessen P, Walhovd KB, 2008 The relationship between diffusion tensor imaging and volumetry as measures of white matter properties. Neuroimage 10.1016/j.neuroimage.2008.06.005.

Fsl, 2006 FMRIB Software Library. Univ, Oxford WWW Document.

Gullett JM, Lamb DG, Porges E, Woods AJ, Rieke J, Thompson P, Jahanshad N, Nir T, Tashima K, Cohen RA, 2018 The impact of alcohol use on frontal white matter in HIV. Alcohol Clin. Exp. Res 42, 1640–1649. [PubMed: 29957870]

Gunning-Dixon FM, Brickman AM, Cheng JC, Alexopoulos GS, 2009 Aging of cerebral white matter: a review of MRI findings. Int. J. Geriatr. Psychiatr 10.1002/gps.2087.

Hoy AR, Ly M, Carlsson CM, Okonkwo OC, Zetterberg H, Blennow K,Sager MA, Asthana S, Johnson SC, Alexander AL, 2017 Microstructural white matter alterations in preclinical Alzheimer's disease detected using free water elimination diffusion tensor imaging. PLoS One 12, e0173982 10.1371/journal.pone.0173982. [PubMed: 28291839]

Hoy AR, Ly M, Carlsson CM, Okonkwo OC, Zetterberg H, Blennow K,Sager MA, Asthana S, Johnson SC, Alexander AL, Bendlin BB, 2017 Microstructural white matter alterations in preclinical Alzheimer's disease detected using free water elimination diffusion tensor imaging. PLoS One. 10.1371/journal.pone.0173982.

Hugenschmidt CE, Peiffer AM, Kraft RA, Casanova R, Deibler AR, Burdette JH, Maldjian JA, Laurienti PJ, 2008 Relating imaging indices of white matter integrity and volume in healthy older adults. Cereb. Cortex 10.1093/cercor/bhm080.

IBM, 2016 SPSS Statistics v24.0.

Jacobsen L. a, Kent M, Lee M, Mather M, 2011 America's aging population. Popul.Bull 66, 1–18.

Jenkinson M, Bannister P, Brady M, Smith S, 2002 Improved optimization for the robust and accurate linear registration and motion correction of brain images. Neuroimage. 10.1016/S1053-8119(02)91132-8.

Jenkinson M, Beckmann CF, Behrens TEJ, Woolrich MW, Smith SM, 2012 FSL. Neuroimage. 10.1016/j.neuroimage.2011.09.015.

Jenkinson M, Smith S, 2001 A global optimisation method for robust affine registration of brain images. Med. Image Anal 10.1016/S1361-8415(01)00036-6.

Ji F, Pasternak O, Ng KK, Chong JSX, Liu S, Zhang L, Shim HY, Loke YM, Tan BY, Venketasubramanian N, Chen CLH, Zhou JH, 2019 White matter microstructural abnormalities and default network degeneration are associated with early memory deficit in Alzheimer's disease continuum. Sci. Rep 10.1038/s41598-019-41363-2.

Jones DK, Horsfield MA, Simmons A, 1999 Optimal strategies for measuring diffusion in anisotropic systems by magnetic resonance imaging. Magn. Reson. Med 42, 515–525. 10.1002/(SICI)1522-2594(199909)42:3<515::AIDMRM14>3.0.CO;2-Q. [PubMed: 10467296]

Jones JD, Kuhn T, Mahmood Z, Singer EJ, Hinkin CH, April D, Jones JD, Kuhn T, Hinkin CH, Thames AD, 2017 Neuropsychology longitudinal intra-individual variability in neuropsychological performance relates to white matter changes in HIV longitudinal intra-individual variability in neuropsychological performance relates to white matter changes in HIV. Neuropsychology 11.

Jovicich J, Czanner S, Han X, Salat D, van der Kouwe A, Quinn B, Pacheco J, Albert M, Killiany R, Blacker D, Maguire P, Rosas D, Makris N, Gollub R, Dale A, Dickerson BC, Fischl B, 2009 MRI-derived measurements of human subcortical, ventricular and intracranial brain volumes: reliability effects of scan sessions, acquisition sequences, data analyses, scanner upgrade, scanner vendors and field strengths. Neuroimage 46, 177–192. 10.1016/j.neuroimage.2009.02.010. [PubMed: 19233293]

Lövdén M, Bergman L, Adolfsson R, Lindenberger U, Nilsson L-G, 2005 Studying individual aging in an interindividual context: typical paths of age-related, dementia-related, and mortality-related cognitive development in old age. Psychol. Aging 20, 303–316. 10.1037/0882-7974.20.2.303. [PubMed: 16029094]

Luo DH, Tseng WYI, Chang YL, 2019 White matter microstructure disruptions mediate the adverse relationships between hypertension and multiple cognitive functions in cognitively intact older adults. Neuroimage. 10.1016/j.neuroimage.2019.04.063.

Madden DJ, Bennett IJ, Burzynska A, Potter GG, Chen N kuei, Song AW, 2012 Diffusion tensor imaging of cerebral white matter integrity in cognitive aging. Biochim. Biophys. Acta (BBA) - Mol. Basis Dis 10.1016/j.bbadis.2011.08.003.

Maier-Hein KH, Westin CF, Shenton ME, Weiner MW, Raj A, Thomann P,Kikinis R, Stieltjes B, Pasternak O, 2015 Widespread white matter degeneration preceding the onset of dementia. Alzheimer's Dementia 11, 485–493. 10.1016/j.jalz.2014.04.518.

Maillard P, Fletcher E, Singh B, Martinez O, Johnson DK, Olichney JM, Farias ST, DeCarli C, 2019 Cerebral white matter free water: a sensitive biomarker of cognition and function. Neurology. 10.1212/WNL.0000000000007449.

Marioni RE, Proust-Lima C, Amieva H, Brayne C, Matthews FE, Dartigues JF, Jacqmin-Gadda H, 2014 Cognitive lifestyle jointly predicts longitudinal cognitive decline and mortality risk. Eur. J. Epidemiol 29, 211–219. 10.1007/s10654-014-9881-8. [PubMed: 24577561]

Montal V, Vilaplana E, Alcolea D, Pegueroles J, Pasternak O, González-Ortiz S,Clarimón J, Carmona-Iragui M, Illán-Gala I, Morenas-Rodríguez E, Ribosa-Nogué R, Sala I, Sánchez-Saudinós M-B, García-Sebastian M, Villanúa J, Izagirre A, Estanga A, Ecay-Torres M, Iriondo A, Clerigue M, Tainta M, Pozueta A, González A, Martínez-Heras E, Llufriu S, Blesa R, Sanchez-Juan P, Martínez-Lage P, Lleó A, Fortea J, 2018 Cortical microstructural changes along the Alzheimer's disease continuum. Alzheimer's Dementia. 10.1016/J.JALZ.2017.09.013.

Morey RA, Petty CM, Xu Y, Pannu Hayes J, Wagner HR, Lewis DV, LaBar KS, Styner M, McCarthy G, 2009 A comparison of automated segmentation and manual tracing for quantifying hippocampal and amygdala volumes. Neuroimage 45, 855–866. 10.1016/j.neuroimage.2008.12.033. [PubMed: 19162198]

Nasreddine Z, Phillips N, Bédirian V, Charbonneau S, Whitehead V, Colllin I, Cummings J, Chertkow H, 2005 The Montreal Cognitive Assessment, MoCA: a brief screening tool for mild cognitive impairment. J. Am. Geriatr. Soc 53, 695–699. 10.1111/j.1532-5415.2005.53221.x. [PubMed: 15817019]

O 'Shea DM, Fieo R, Woods A, Williamson J, Porges E, Cohen R, 2018 Discrepancies between crystallized and fluid ability are associated with frequency of social and physical engagement in community dwelling older adults. J. Clin. Exp. Neuropsychol 10.1080/13803395.2018.1452195.

Ofori E, Pasternak O, Planetta PJ, Li H, Burciu RG, Snyder AF, Lai S, Okun MS, Vaillancourt DE, 2015 Longitudinal changes in free-water within the substantia nigra of Parkinson's disease. Brain 138, 2322–2331. 10.1093/brain/awv136. [PubMed: 25981960]

Özarslan E, Vemuri BC, Mareci TH, 2005 Generalized scalar measures for diffusion MRI using trace, variance, and entropy. Magn. Reson. Med 53, 866–876. 10.1002/mrm.20411. [PubMed: 15799039]

Pasternak O, Koerte IK, Bouix S, Fredman E, Sasaki T, Mayinger M, Helmer KG, Johnson AM, Holmes JD, Forwell LA, Skopelja EN, Shenton ME, Echlin PS, 2014 Hockey Concussion Education Project, Part 2. Microstructural white matter alterations in acutely concussed ice hockey players: a longitudinal free-water MRI study. J. Neurosurg 120, 873–881. 10.3171/2013.12.JNS132090. [PubMed: 24490785]

Pasternak O, Kubicki M, Shenton ME, 2016 In vivo imaging of neuroinflammation in schizophrenia. Schizophr. Res 10.1016/j.schres.2015.05.034.

Pasternak O, Sochen N, Gur Y, Intrator N, Assaf Y, 2009 Free water elimination and mapping from diffusion MRI. Magn. Reson. Med 62, 717–730. 10.1002/mrm.22055. [PubMed: 19623619]

Pasternak O, Westin C-F, Bouix S, Seidman LJ, Goldstein JM, Woo T-UW, Petryshen TL, Mesholam-Gately RI, McCarley RW, Kikinis R, Shenton ME, Kubicki M, 2012 Excessive extracellular volume reveals a neurodegenerative pattern in schizophrenia onset. J. Neurosci 32, 17365–17372. 10.1523/JNEUROSCI.2904-12.2012. [PubMed: 23197727]

Pasternak O, Westin CF, Dahlben B, Bouix S, Kubicki M, 2015 The extent of diffusion MRI markers of neuroinflammation and white matter deterioration in chronic schizophrenia. Schizophr. Res 161, 113–118. 10.1016/j.schres.2014.07.031. [PubMed: 25126717]

Poustchi-Amin M, Mirowitz S. a, Brown JJ, McKinstry RC, Li T, 2001 Principles and applications of echo-planar imaging: a review for the general radiologist. Radiographics 21, 767–779. 10.1148/radiographics.21.3.g01ma23767. [PubMed: 11353123]

R Development Core Team, 2016 R: A Language and Environment for Statistical Computing. R Found. Stat. Comput Vienna Austria 0, ISBN 3-900051-07-0. 10.1038/sj.hdy.6800737.

Raz N, Lindenberger U, Rodrigue KM, Kennedy KM, Head D, Williamson A,Dahle C, Gerstorf D, Acker JD, 2005 Regional brain changes in aging healthy adults: general trends, individual differences and modifiers. Cerebr. Cortex 10.1093/cercor/bhi044.

Rydhög A, Pasternak O, Ståhlberg F, Ahlgren A, Knutsson L, Wirestam R, 2019 Estimation of diffusion, perfusion and fractional volumes using a multi-compartment relaxation-compensated intravoxel incoherent motion (IVIM)signal model. Eur. J. Radiol. Open 10.1016/j.ejro.2019.05.007.

Rydhög AS, Szczepankiewicz F, Wirestam R, Ahlgren A, Westin CF, Knutsson L, Pasternak O, 2017 Separating blood and water: perfusion and free water elimination from diffusion MRI in the human brain. Neuroimage. 10.1016/j.neuroimage.2017.04.023.

Salat DH, Kaye JA, Janowsky JS, 1999 Prefrontal gray and white matter volumes in healthy aging and Alzheimer disease. Arch. Neurol 10.1001/archneur.56.3.338.

Salthouse TA, 1998 Independence of age-related influences on cognitive abilities across the life span. Dev. Psychol 10.1037/0012-1649.34.5.851.

Schmahmann JD, Pandya DN, 2009 Fiber Pathways of the Brain, Fiber Pathways of the Brain. 10.1093/acprof:oso/9780195104233.001.0001.

Templeton GF, 2011 A two-step approach for transforming continuous variables to normal: implications and recommendations for IS research. Commun. Assoc. Inf. Syst 28, 41–58.

Vos SB, Jones DK, Viergever MA, Leemans A, 2011 Partial volume effect as a hidden covariate in DTI analyses. Neuroimage. 10.1016/j.neuroimage.2011.01.048.

Weintraub S, Dikmen SS, Heaton RK, Tulsky DS, Zelazo PD, Bauer PJ, Carlozzi NE, Slotkin J, Blitz D, Wallner-Allen K, Fox NA, Beaumont JL, Mungas D, Nowinski CJ, Richler J, Deocampo JA, Anderson JE, Manly JJ, Borosh B, Havlik R, Conway K, Edwards E, Freund L, King JW, Moy C, Witt E, Gershon RC, 2013 Cognition assessment using the NIH Toolbox. Neurology 80, S54–64. 10.1212/WNL.0b013e3182872ded. [PubMed: 23479546]

Weston PSJ, Simpson IJA, Ryan NS, Ourselin S, Fox NC, 2015 Diffusion imaging changes in grey matter in Alzheimer's disease: a potential marker of early neurodegeneration. Alzheimer's Res. Ther 10.1186/s13195-015-0132-3.

Wickham H, 2017 ggplot2: elegant graphics for data analysis. J. Stat. Software 10.18637/jss.v080.b01.

Woods AJ, Cohen RA, Pahor M, 2013 Cognitive frailty: frontiers and challenges.J. Nutr. Health Aging 17, 741–743.

Woods AJ, Mark VW, Pitts AC, Mennemeier M, 2011 Pervasive cognitive impairment in acute rehabilitation inpatients without brain injury. Pharm. Manag. PM R 3, 426–432. 10.1016/j.pmrj.2011.02.018 quiz 432.

Yendiki A, 2011 Automated probabilistic reconstruction of white-matter pathways in health and disease using an atlas of the underlying anatomy. Front. Neuroinf 5, 1–12. 10.3389/fninf.2011.00023.

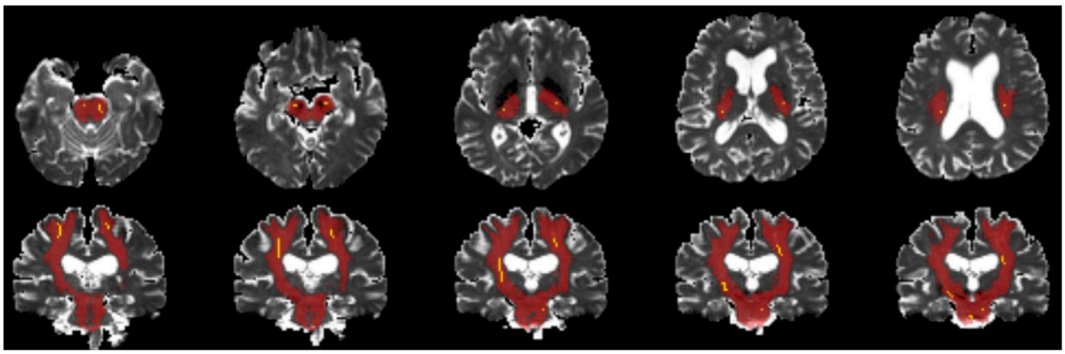

Fig. 1.

A representative bilateral corticospinal tract pathway depicting the differential size and location of the 99th percentile probability pathway (bright yellow) as compared to the standard TRACULA pathway output (red).

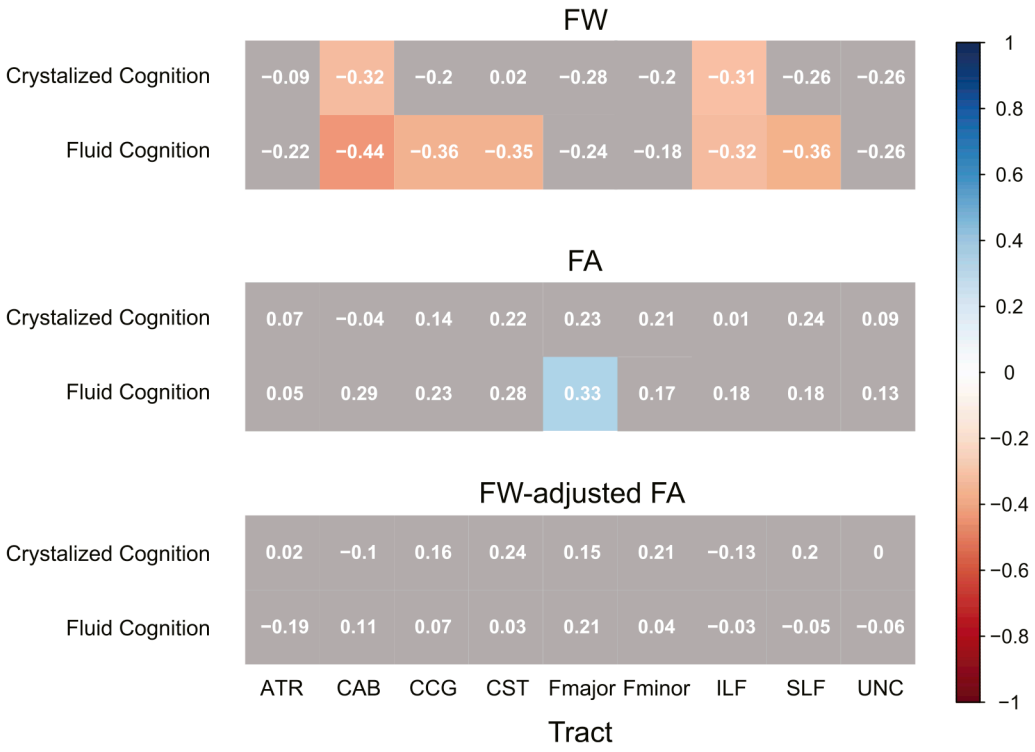

Fig. 2.

Partial correlogram displaying the partial correlation between age-, education-, and gender-adjusted diffusion metrics and age-, education-, and gender-adjusted cognitive performance. *Note:* FW = Free Water, FA = Fractional Anisotropy, FW-adjusted FA = Free Water adjusted Fractional Anisotropy; ATR = Anterior Thalamic Radiation; CAB = Cingulate Gyrus, angular bundle; CCG = Cingulate Gyrus, cingulum bundle; CST = corticospinal tract; Fmajor = Forceps Major, corpus callosum; Fminor = Forceps Minor, corpus callosum; ILF = inferior longitudinal fasciculus; SLF = superior longitudinal fasciculus; UNC = uncinate fasciculus.

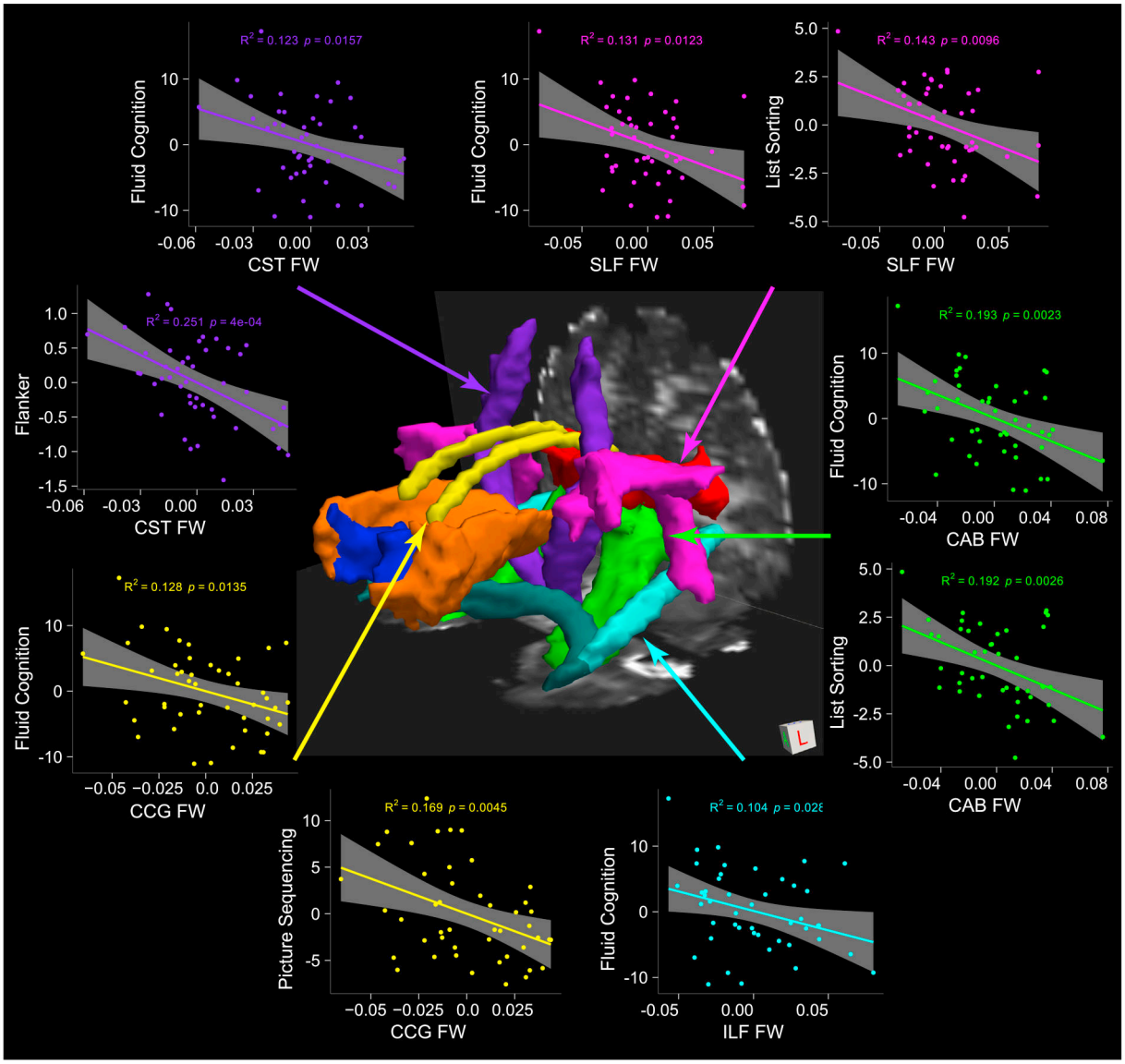

Fig. 3.

Three-dimensional representation of the larger tract from which the 99th percentile white matter pathway was extracted for diffusion metric analysis along with the associated cognitive index and/or subtest for each pathway. *Note:* Only significant associations displayed. All values represent the measure of interest adjusted for age, gender, and education. FW = Free Water, FA = Fractional Anisotropy, FW-adjusted FA = Free Water adjusted Fractional Anisotropy; ATR = Anterior Thalamic Radiation; CAB = Cingulate Gyrus, angular bundle; CCG = Cingulate Gyrus, cingulum bundle; CST = corticospinal tract; Fmajor = Forceps Major, corpus callosum; Fminor = Forceps Minor, corpus callosum; ILF = inferior longitudinal fasciculus; SLF = superior longitudinal fasciculus; UNC = uncinate fasciculus.

Table 1

Sample demographics.

Variable	Total Mean (SD) N = 47	Male Mean (SD) N = 20	Female Mean (SD) N = 27
Age	74.4 (5.4)	73.8 (4.8)	74.9 (5.8)
Highest Educational Level	16.6 (2.4)	16.6 (2.7)	16.7 (2.1)
Right-Handed	95.7%	95.0%	96.3%
Race			
Caucasian	95.8%	100.0%	92.6%
African-American	2.1%	0.0%	3.7%
Latino	2.1%	0.0%	3.7%
MoCA Total Score	25.8 (2.5) *	24.6 (1.9)	26.7 (2.5)
NIH Toolbox Crystallized Performance	115.8 (18.5)	111.1 (20.3)	119.2 (16.6)
NIH Toolbox Fluid Performance	100.0 (12.5)	97.7 (12.2)	101.6 (12.7)

* Female performance significantly higher than male $p < .01$.

Note: Adjusted Scaled Scores have a mean of 100 and standard deviation of 15; MoCA = Montreal Cognitive Assessment; NIH Toolbox Crystallized Performance is comprised of the Picture Vocabulary Test and the Oral Reading Recognition Test; NIH Toolbox Fluid Performance is comprised of Dimensional Change Card Sort, Flanker, Picture Sequence Memory, List Sorting, and Pattern Comparison tasks.

Table 2

Association of age with diffusion metrics using TraCULA (N = 47).

		R^2	β_{age}	p-val			R^2	β_{age}	p-val			R^2	β_{age}	p-val
Free Water	ATR	0.20	0.441	0.003 *	Fractional Anisotropy	ATR	0.06	−0.143	0.343	Free Water-adjusted Fractional Anisotropy	ATR	0.02	−0.046	0.765
	CAB	0.12	0.316	0.038		CAB	0.03	−0.043	0.783		CAB	0.02	0.050	0.748
	CCG	0.03	0.022	0.883		CCG	0.02	−0.050	0.746		CCG	0.03	−0.020	0.897
	CST	0.08	0.204	0.176		CST	0.09	−0.042	0.776		CST	0.09	0.047	0.749
	Fmajor	0.10	0.011	0.942		Fmajor	0.05	−0.127	0.401		Fmajor	0.07	−0.136	0.368
	Fminor	0.05	0.215	0.169		Fminor	0.03	−0.024	0.877		Fminor	0.04	0.114	0.463
	ILF	0.14	0.302	0.038		ILF	0.04	−0.145	0.351		ILF	0.01	−0.087	0.581
	SLF	0.12	0.347	0.021		SLF	0.08	0.052	0.728		SLF	0.17	0.262	0.069
	UNC	0.13	0.002	0.302		UNC	0.05	−0.007	0.966		UNC	0.05	0.139	0.367

* survives FDR-correction at $p < .05$;

** survives FDR-correction at $p < .01$.

Note: Covariates included in regression model = years of education, gender; β = Standardized Beta Weight; ATR = Anterior Thalamic Radiation; CAB = Cingulate Gyrus Angular Bundle; CCG = Cingulate Gyrus, cingulum bundle; CST = corticospinal tract; Fmajor = Forceps Major, corpus callosum; Fminor = Forceps Minor, corpus callosum; ILF = inferior longitudinal fasciculus; SLF = superior longitudinal fasciculus; UNC = uncinate fasciculus.

Table 3

Association of free water with fluid cognition in older adults (N = 47).

	NIHTB Fluid Cognition				Subtest Contributions to Fluid Index					Hemispheric Contributions to Subtest Performance				
	R^2	β	p	p (FDR)		R^2	β	p	p (FDR)		R^2	β	p	p (FDR)
CAB (bilateral)	0.35	−0.42	0.003*	0.027	CAB (bilateral)	0.35		0.003*	0.027					
Hemispheric Model	0.37		0.002*	0.048	List Sorting		−0.44	0.003*	0.015	List Sorting	0.30		0.003*	0.027
Left CAB		−0.47	0.004*	0.048						Left CAB		−0.44	0.006	0.069
Right CAB		−0.22	0.194	0.235						Right CAB		−0.23	0.153	0.224
CCG (bilateral)	0.29	−0.33	0.017*	0.045	CCG (bilateral)	0.29		0.017*	0.045					
Hemispheric Model	0.31		0.009*	0.048	Picture Seq.		−0.41	0.006*	0.030	Picture Seq.	0.24		0.006*	0.030
Left CCG		−0.26	0.118	0.203						Left CCG		−0.25	0.099	0.176
Right CCG		−0.42	0.012*	0.048						Right CCG		−0.46	0.002*	0.032
CST (bilateral)	0.28	−0.33	0.020*	0.045	CST (bilateral)	0.28		0.020*	0.045					
Hemispheric Model	0.30		0.013*	0.048	Flanker		−0.49	0.001**	0.005	Flanker	0.35		0.001**	0.005
Left CST		−0.28	0.096	0.192						Left CST		−0.40	0.012	0.064
Right CST		−0.33	0.041	0.109						Right CST		−0.45	0.003*	0.032
ILF (bilateral)	0.25		0.035	0.063	ILF (bilateral)	0.25		0.035	0.063					
Hemispheric Model	0.33		0.006*	0.048	*None*	–	–	–	–	*None*	–	–	–	–
Left ILF		−0.20	0.206	0.235	–	–	–	–	–	–	–	–	–	–
Right ILF		−0.42	0.006*	0.048	–	–	–	–	–	–	–	–	–	–
SLF (bilateral)	0.30	−0.35	0.016*	0.045	SLF (bilateral)	0.30		0.016*	0.045					
Hemispheric Model	0.31		0.009*	0.048	List Sorting		−0.38	0.012*	0.033	List Sorting	0.25		0.012*	0.033
Left SLF		−0.40	0.011*	0.048						Left SLF		−0.38	0.013	0.069
Right SLF		−0.30	0.065	0.149						Right SLF		−0.34	0.028	0.112

* survives FDR-correction at $p < .05$;

** survives FDR-correction at $p < .01$.

Note: Mean free water is represented across the 99% probabilistic connectivity white matter tract data with regression covariates age, education, and gender. Only values displayed for pathways significant prior to FDR correction. ATR = Anterior Thalamic Radiation; CAB = Cingulate Gyrus, angular bundle; CCG = Cingulate Gyrus, cingulum bundle; CST = corticospinal tract; SLF = superior longitudinal fasciculus.